

Quantum criticality driven by the cavity coupling in the Rabi-dimer model

Shujie Cheng,¹ He-Guang Xu,² Xueying Liu,¹ and Gao Xianlong^{1,*}

¹*Department of Physics, Zhejiang Normal University, Jinhua 321004, China*

²*School of Physics, Dalian University of Technology, Dalian 116024, China*

(Dated: November 8, 2022)

The superradiant phase transition (SPT) controlled by the interacting strength between the two-level atom and the photons has been a hot topic in the Rabi model and the Rabi-dimer model. The latter describes two Rabi cavities coupled with an inter-cavity hopping parameter. Moreover, the SPT in the Rabi-dimer model is found to be the same universal class that in the Rabi model by investigating the correlation-length critical exponent. In this paper, we are concerned about whether the inter-cavity hopping parameter between two Rabi cavities (i.e., the Rabi-dimer model) will induce the SPT and to which the universal class of the phase transition belongs. We analytically derive the phase boundary of the SPT and investigate the ground-state properties of the system. We uncover that the inter-cavity induced SPT can be apparently understood from the ground-state energy and the ground-state photon population, as well as the ground-state expectation value of the squared anti-symmetric mode. From the scaling analysis of the fidelity susceptibility, we numerically verify that the SPT driven by the cavity coupling belongs to the same universal class as the one driven by the atom-cavity interaction. Our work enriches the studies on the SPT and its critical behaviors in the Rabi-dimer model.

PACS numbers:

I. INTRODUCTION

The quantum system involving single-mode cavity interacting with a cloud of two-level atoms can be described by the Dicke model [1]. When the interaction strength exceeds the critical value, the system will undergo from a normal phase to a superradiant phase. This quantum behavior, is known as the superradiant phase transition (SPT). During the decades, the investigation on the SPT has involved in many experimental mediums, ranging from the atomic or molecular clouds [2–8], nuclei [9], Rydberg atomic gas [10–13], to superconducting qubits [14], and semiconductors [15, 16]. Recently, some attentions from the perspective of theoretical schemes [17, 18] and experimental engineering [19–23] are focused on how to employ the superradiant feature to design a new generation of extremely stable lasers.

In fact, beyond the multiatomic system, there appears superradiant phenomenon as well. A representative system is the quantum Rabi model [24, 25], which describes a single two-level atom interacting with a single-mode cavity. To investigate the SPT in the Rabi model, it is necessary to obtain the energy spectrum information and wavefunctions. However, it has not been clear for a long time whether the Rabi model has analytical solutions of the eigenvalues and wavefunctions. More are focused on the aspects of quasi-exact solutions [26, 27] and the analytically explicit but approximate studies [28–33]. However, Braak extracted the exact solution of the Rabi model [34] in virtue of the Bargmann space [35] and Chen et al. obtained the exact solution of a two-photon Rabi model by using the Bogoliubov transformations [36]. Regarding the SPT, it is clear that the superradiance appears when the ratio of the atomic frequency and the photonic frequency approaches the thermodynamic limit [37–42], by which the universal dynamics of the Rabi model is well studied [43]. Here, the the thermodynamic limit in these models refers to the frequency ratio tending to infinity. Recently, this finding has stimulated the researches on the SPT in other photonic systems [44–49].

Among the studies on the SPT, there exist interests in studying the quantum criticality of the above-mentioned systems. Wei et al. investigated that in the Rabi model the fidelity susceptibility presents finite-frequency scaling behaviors near the SPT point [47], and the correlation-length critical exponent (CLCE) is calculated as $\nu = 3/2$ [43, 47]. The Rabi-dimer (RD) model is a general extension of the Rabi model in the multi-cavity system, which describes two Rabi cavities coupled by an inter-cavity hopping strength [46]. For the RD system, more attention is focused on the SPT induced by the atom-cavity interacting strength. Mao et al. found that the asymptotic behaviors of the expectation value of canonical coordinate and the first-order derivative of entanglement entropy conform to the same scaling function, and the extracted critical exponent agrees with that of the single Rabi model [48]. Even

*Corresponding author: gaoxl@zjnu.edu.cn

including the \mathbf{A}^2 -term in the RD model, the CLCE remains the same [49]. Interestingly, we notice that the CLCE of the Rabi and RD models is the same as the one in the Dicke model [50, 51] and the Lipkin-Meshkov-Glick (LMG) model [52–54]. It means that the known phase transitions in the normal Rabi model, RD model, Dicke model, and the LMG model all belong to the same universal class. However, in the RD model, the study on the relationship between the inter-cavity hopping strength and the SPT is lacking. Accordingly, whether such an inter-cavity hopping-dominated SPT belongs to the same universal class remains unknown.

To answer the above questions, we take the following strategies: First of all, we introduce the RD model and investigate the SPT by analyzing how the ground-state (GS) energy and GS photon population, as well as the squared anti-symmetric normal mode response to the inter-cavity hopping strength in Sec. II. Furthermore, we study the quantum criticality and extract the CLCE by analyzing the scaling behavior of the fidelity susceptibility in Sec. III. A summary is presented in Sec. IV.

II. RABI-DIMER MODEL AND SPT

The general Hamiltonian ($\hbar = 1$) of the quantum RM model is written as

$$H(J)/\omega = H_0 + JH_1, \quad (1)$$

where H_0 denotes the Hamiltonian of two equivalent cavities and each of the cavities is described by the Rabi model. Here, the equivalent cavities refer to that the photonic frequency, atomic frequency, and photon-atom coupling strength of two cavities are the same, equaling to ω , Ω , and λ , respectively.

By introducing the dimensionless parameters $\eta = \Omega/\omega$ and $g = 2\lambda/\sqrt{\Omega\omega}$, H_0 reads

$$H_0 = \sum_{i=L,R} a_i^\dagger a_i + \frac{\eta}{2} \sigma_i^z - \frac{g\sqrt{\eta}}{2} (a_i + a_i^\dagger) \sigma_i^x, \quad (2)$$

where L and R are the notations of two cavities, and a^\dagger and a are bosonic operators.

H_1 is the driving Hamiltonian coupling the two cavities with the inter-cavity hopping strength J , defined as

$$H_1 = (a_L^\dagger + a_L) (a_R^\dagger + a_R). \quad (3)$$

To obtain the phase boundary of the inter-cavity coupling driven SPT in the ground state, the Hamiltonian in Eq. (1) is written as

$$\mathcal{H} = \frac{H}{\Omega} \equiv \frac{1}{\eta} H_0 + \frac{J}{\eta} H_1. \quad (4)$$

Replacing the creation and annihilation operators by the renormalized canonical coordinates (i.e., $x_i = (a_i^\dagger + a_i)/\sqrt{2\eta}$ and $p_i = i(a_i^\dagger - a_i)\sqrt{\eta/2}$), we have

$$\mathcal{H} = \frac{1}{2} \sum_{i=L,R} \left[x_i^2 + \frac{p_i^2}{\eta^2} + \sigma_i^z - \sqrt{2}g\sigma_i^x x_i \right] + 2Jx_Lx_R, \quad (5)$$

and the symmetric (x_+) and anti-symmetric (x_-) normal modes satisfy $x_\pm = (x_L \pm x_R)/\sqrt{2}$ [48].

In the large- η limit ($\eta \rightarrow \infty$), \mathcal{H} further becomes

$$\mathcal{H} = \frac{1}{2} \sum_{i=L,R} \left[x_i^2 + \sigma_i^z - \sqrt{2}g\sigma_i^x x_i \right] + 2Jx_Lx_R, \quad (6)$$

whose energies are

$$E_\pm(x_L, x_R) = \frac{1}{2} \sum_{i=L,R} \left(x_i^2 \pm \sqrt{1 + 2g^2x_i^2} \right) + 2Jx_Lx_R. \quad (7)$$

The low-energy branch $E_-(x_L, x_R)$ reflects the ground-state properties of the system. Truncating the expansion of $E_-(x_L, x_R)$ to the quadratic term ($\mathcal{O}(x_i^4)$), we have

$$E_- = \frac{1}{2} \psi^T \Lambda \psi, \quad (8)$$

with $\Lambda = \begin{pmatrix} 1 - g^2 & 2J \\ 2J & 1 - g^2 \end{pmatrix}$ and $\psi = (x_L, x_R)^T$.

The eigenvalues λ_{\pm} of the matrix Λ are $\lambda_{\pm} = 1 - g^2 \pm 2J$. According to the Refs. [48, 49], the phase boundary can be extracted from $\lambda_- = 0$. Accordingly, the critical point J_c is obtained as $J_c = (1 - g^2)/2$. From the expression of J_c and the phase diagram in Fig. 1(a), we intuitively know that the critical point of SPT gradually tends to zero with the increase of g .

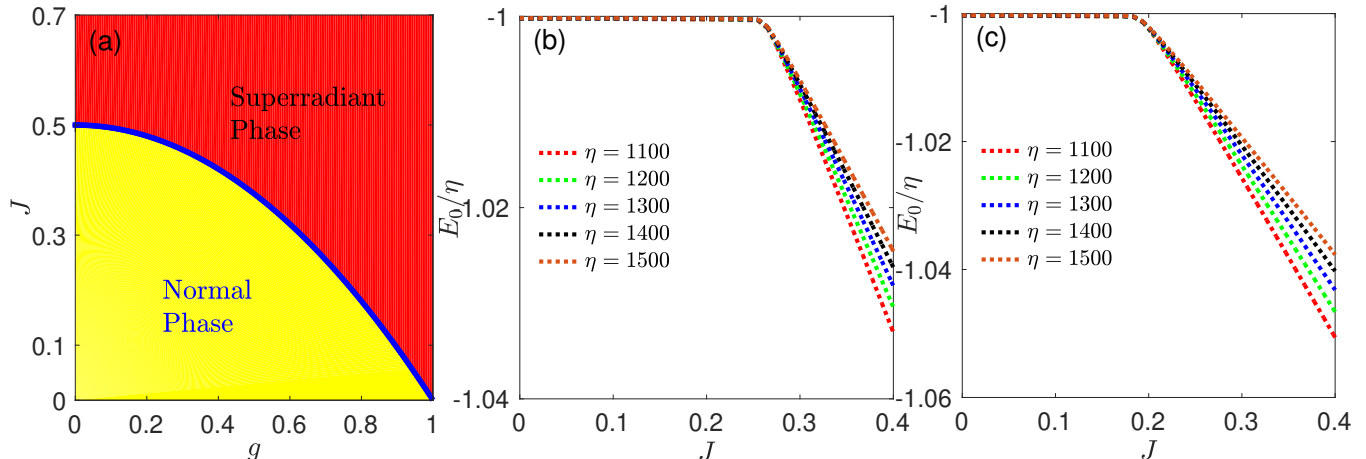


Figure 1: (Color Online) (a) Phase diagram in the J - g parameter space. The blue solid line indicates the analytically obtained phase boundary ($J_c = (1 - g^2)/2$), separating the normal phase (yellow region) from the superradiant one (red region). The GS energy E_0 as a function of the inter-cavity hopping strength J with $g = 0.7$ (b) and $g = 0.8$ (c). The colors of the curves correspond to different η .

To further understand the properties of SPT, in the following, we investigate how the ground state energy, the number of ground state photons, and the GS expectation value of the squared anti-symmetric normal mode response to the cavity coupling. The Hamiltonian matrix of the RD model is constructed by the Fock states and the GS energy (E_0) and the GS wave function is calculated by the Lanczos method. Without loss of generality, two typical cases with $g = 0.7$ and $g = 0.8$ are chosen for the numerical analysis. Other parameter spaces are tested supporting the SPT we found. In appendix we study the system with smaller $g = 0.5$. In this case, the SPT phenomenon remains, and the quantum criticality is the same as the ones of $g=0.7$ and 0.8 (see details in A). At first, we present the numerical results of the GS energy E_0 as the varying of the hopping strength J for various $\eta = 1100, 1200, 1300, 1400, 1500$ in Figs. 1(b) and 1(c), with atom-cavity interacting strengths $g = 0.7$ and $g = 0.8$, respectively. Intuitively, one can see an obvious phenomenon that when J is small, E_0 is stable at $E_0 \approx -\eta$, and when J exceeds a critical point, E_0 moves towards lower values. This abrupt transition behavior of the GS energy implies the appearance of the SPT in this RD model. When $E_0 \approx -\eta$, the system is in the normal phase while it is superradiant when E_0 is much lower than $-\eta$. Besides, we notice that the transition point in the $g = 0.8$ case is smaller than that in the $g = 0.7$ case. The stronger atom-cavity interaction will make the system superradiant.

Then, we study the response of the GS photon populations $\langle a_{L(R)}^\dagger a_{L(R)} \rangle$ to the hopping strength J . By considering the above mentioned η and the two cases where $g = 0.7$ and $g = 0.8$, we plot the $\langle a_{L(R)}^\dagger a_{L(R)} \rangle$ as a function of J in Figs. 2(a) and 2(b), respectively. Intuitively, there appears a significant feature that signals the occurrence of the SPT. Namely, a large number of photons erupt in the cavities when the hopping strength J exceeds the critical point [46], before which the photon population approaches zero, corresponding to the normal phase. Due to the parity symmetry, the photon populations of the two cavities vary synchronously as the hopping strength J increases. It can be interpreted why the photon population presents different behavior before and after the SPT according to the change of the GS energy. When the system is in the normal phase, the GS energy is stable at $E_0 \approx -\eta$, without radiating photon. Therefore, the GS photon populations of the two cavities both approach zero. When the system is in the superradiant phase, due to the dramatic decrease of the GS energy with increasing J , macroscopic excitation of photons emerges. Figures 2(c) ($g = 0.7$) and 2(d) ($g = 0.8$) present the change of the GS expectation value of the squared anti-symmetric normal mode $\langle x_-^2 \rangle$ with J . This quantity serves as the order parameter to distinguish the superradiant phase from the normal phase. Intuitively, the variational tendency is similar to that of the GS photon population. Before the SPT, $\langle x_-^2 \rangle$ approaches zero, whereas it tends to finite values when SPT happens. The

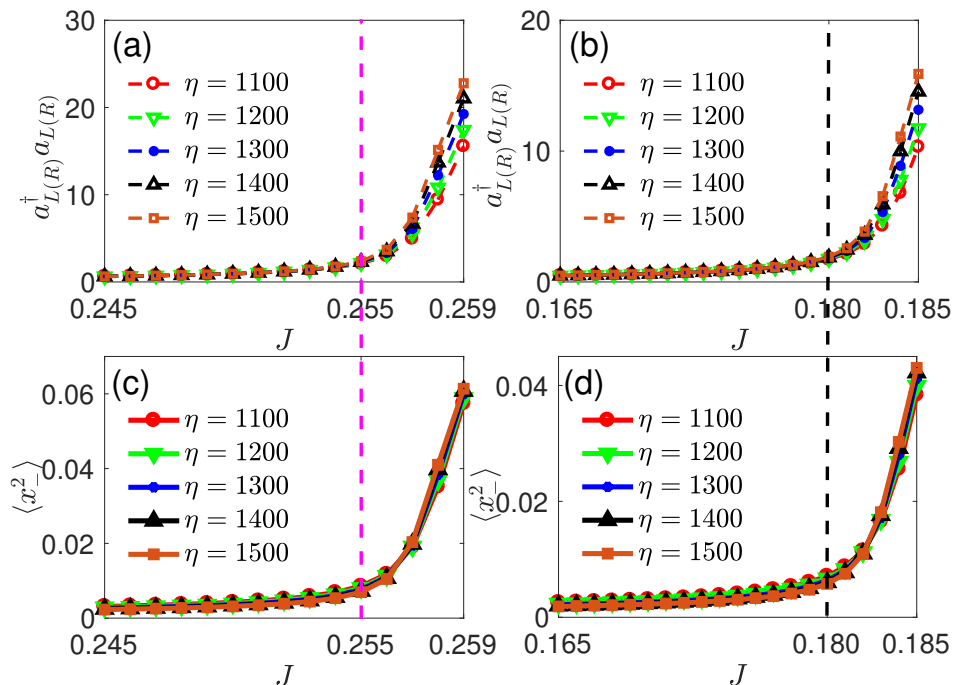


Figure 2: (Color Online) Upper panel: The GS photon populations $a_L^\dagger a_L$ and $a_R^\dagger a_R$ as a function of the inter-cavity hopping strength J with $g = 0.7$ (a) and with $g = 0.8$ (b). Lower panel: The expectation value of the squared anti-symmetric normal mode $\langle x_-^2 \rangle$ as a function of J with $g = 0.7$ (c) and with $g = 0.8$ (d). The colors of the curves correspond to different η . The dotted magenta reference lines in (a) and (c) denote the exact phase boundaries for $g = 0.7$. The dotted black reference lines in (b) and (d) denote the ones for $g = 0.8$.

superradiant phenomenon can be interpreted by the two-fold broken parity as well. On the one hand, the known shift of the oscillators to nonzero expectation values of x_-^2 leads to the nonzero $\langle a_{L(R)}^\dagger a_{L(R)} \rangle$, but on the other, in the RD model, the breaking of the permutation system between cavities leads to the nonzero $\langle x_-^2 \rangle$. In the above analyses, we have shown that the inter-cavity hopping parameter in the RD model will lead to the SPT as well, which can be characterized by the behaviors of the GS energy and the GS photon population, as well as the GS expectation value of the anti-symmetric normal mode. In the following, we study the critical behavior and extract the CLCE by employing the fidelity susceptibility.

III. FIDELITY, FIDELITY SUSCEPTIBILITY AND QUANTUM CRITICALITY

The concept of fidelity originates from the quantum information theory [55] and is usually used to study the critical phenomenon. The definition of the ground-state fidelity $F(J, \delta J)$ is presented as [56–58]

$$F(J, \delta J) = |\langle \psi_0(J) | \psi_0(J + \delta J) \rangle|, \quad (9)$$

which is the overlap of two ground states $\psi_0(J)$ and $\psi_0(J + \delta J)$ with the driving parameter having a small amount deviation δJ . When $\delta J \rightarrow 0$, the fidelity susceptibility (FS) is defined as [59]

$$\chi_F = \lim_{\delta J \rightarrow 0} \frac{-2 \ln F(J, \delta J)}{(\delta J)^2}. \quad (10)$$

If considering the contribution of the excited states to the fidelity, the FS can be alternatively calculated by $\chi_F(J) = \sum_{n \neq 0} \frac{|\langle \psi_n(J) | H_1 | \psi_0(J) \rangle|^2}{[E_n(J) - E_0(J)]^2}$ [59, 60], where the wave function $\psi_n(J)$ and eigenenergy E_n satisfy $H(J) |\psi_n(J)\rangle = E_n(J) |\psi_n(J)\rangle$. This quantity is usually employed to characterize the quantum phase transition and the quantum critical scaling behavior, and to extract the critical exponents [61, 62]. If we calculate the FS according to the alternative definition, we need to ensure the convergence of the excited states. However, it requires a large truncation

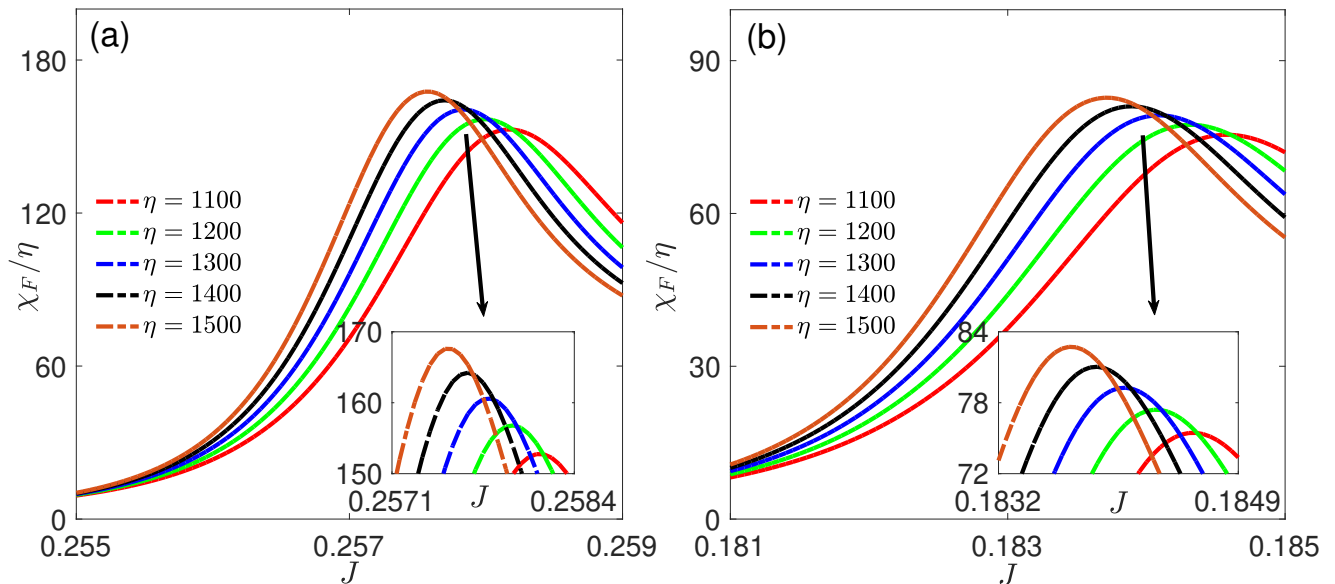


Figure 3: (Color online) The fidelity susceptibility χ_F (rescaled by η) as a function of the control parameter J . (a) $g = 0.7$. (b) $g = 0.8$. The colors of the curves correspond to different η . The inset represents the zoom around the peaks of χ_F/η . Other involved parameter is $\delta J = 5 \times 10^{-5}$.

number and takes heavy computer time. Instead, a large truncation number can be avoided if we care only about the convergence of the ground state. Therefore, in our numerical simulation, we employ Eq. (10) to compute the FS. The truncation number is taken at $N_{cut} = 80$, which is sufficient for the present purpose (See A for the analysis of a larger truncation).

We concentrate on the critical behavior of the FS and extract the CLCE by performing the finite-frequency scaling analysis. Referring to the definition of the finite-size scaling of the FS approaching the critical point that $\chi_F(J_{max}) \propto L^\mu$ [54, 58, 62], the finite-frequency scaling of the FS around the transition point is given as

$$\chi_F(J_{max}) \propto \eta^\mu, \quad (11)$$

where μ is the critical exponent of FS and J_{max} is the critical point at which the χ_F peaks.

For a finite-size system, the FS satisfies such a scaling behavior [62, 63]

$$\chi_F(J) = \eta^{2/\nu} f[\eta^{1/\nu}(J - J_{max})], \quad (12)$$

where ν is the CLCE and $f(x)$ is the scaling function.

In the following, we study the quantum critical behavior. With the exact diagonalization method, we numerically obtain the full energy spectrum and its corresponding wave function. By employing Eq. (10) and considering $\delta J = 5 \times 10^{-5}$, we plot the FS as a function of the control parameter J for different η , which are plotted in Figs. 3(a) and 3(b), respectively. The corresponding g are $g = 0.7$ and $g = 0.8$, respectively. The inset represents the zoom around the peaks of χ_F/η . The FS peaks at the critical point, showing the occurrence of the SPT. Besides, intuitively, one can see that the ratio η plays a similar role as that of the size of the system in common phase transitions. The maximal value of FS varies with the increasing η . Furthermore, the tendency of the χ_F/η is in accord with that of the single Rabi model [47], namely, $\chi_F(J_{max})$ increases as the η increases.

To verify the above conjecture, we first investigate the finite-frequency scaling of the FS near the critical point. Figures 4(a) and 4(b) shows the logarithm of the maximal value of the fidelity susceptibility $\ln(\chi_F^{max})$ (the red open circles show) as a function of $\ln(\eta)$, corresponding to the cases with $g = 0.7$ and $g = 0.8$, respectively. Here, $\delta = 10^{-5}$ is considered in the calculations. After performing a linear fitting on these data, we find that the slope of the fitting curve satisfies 1.300 ± 0.001 (the black line shows) for $g = 0.7$. From the scaling form in Eq. (11), for $g = 0.7$, the critical exponent of the FS near the critical point is $\mu = 2/\nu = 1.300 \pm 0.001$, from which we extract the CLCE as $\nu|_{g=0.7} = 1.539 \pm 0.001$. For $g = 0.8$, the slope of the fitting curve presents the exponent $\mu = 2/\nu = 1.297 \pm 0.002$. Therefore, the CLCE of the case with $g = 0.8$ is $\nu|_{g=0.8} = 1.542 \pm 0.002$. The numerically obtained μ and ν are close to the exact results [43, 45], equal to $4/3$ and $3/2$, respectively. Noting that there are precedents where the numerical exponent deviates from the theoretical value [47, 49, 54]. Our results imply that the inter-cavity-hopping-parameter

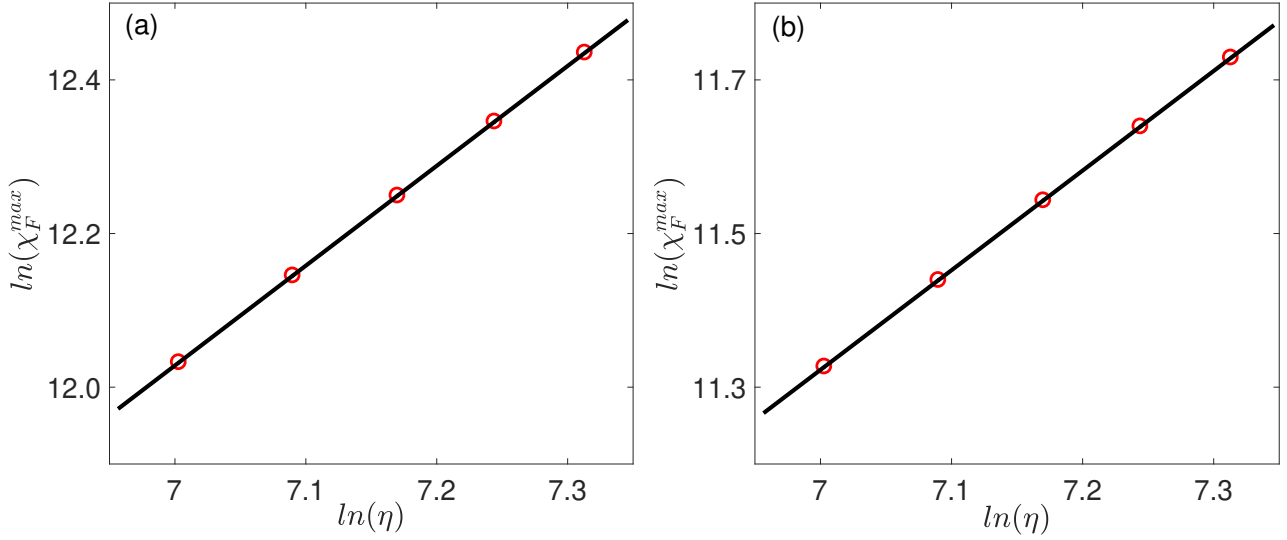


Figure 4: (Color online) Finite-frequency scaling of the logarithm of the maximal value of the fidelity susceptibility $\ln(\chi_F^{max})$ as a function of $\ln(\eta)$ for $g = 0.7$ in (a) and for $g = 0.8$ in (b). The red open circles are the numerical result and the black solid lines are the linear fitting of the numerically obtained data. In (a), the slope of the fitting curve presents the scaling exponent of the fidelity susceptibility $\mu = 1.300 \pm 0.001$. In (b), the slope of the fitting curve presents the scaling exponent $\mu = 1.297 \pm 0.002$. The involved parameter is $\delta J = 10^{-5}$.

dominated SPT has a similar quantum scaling behavior as the SPT driven by the cavity-atom interaction in the single Rabi model.

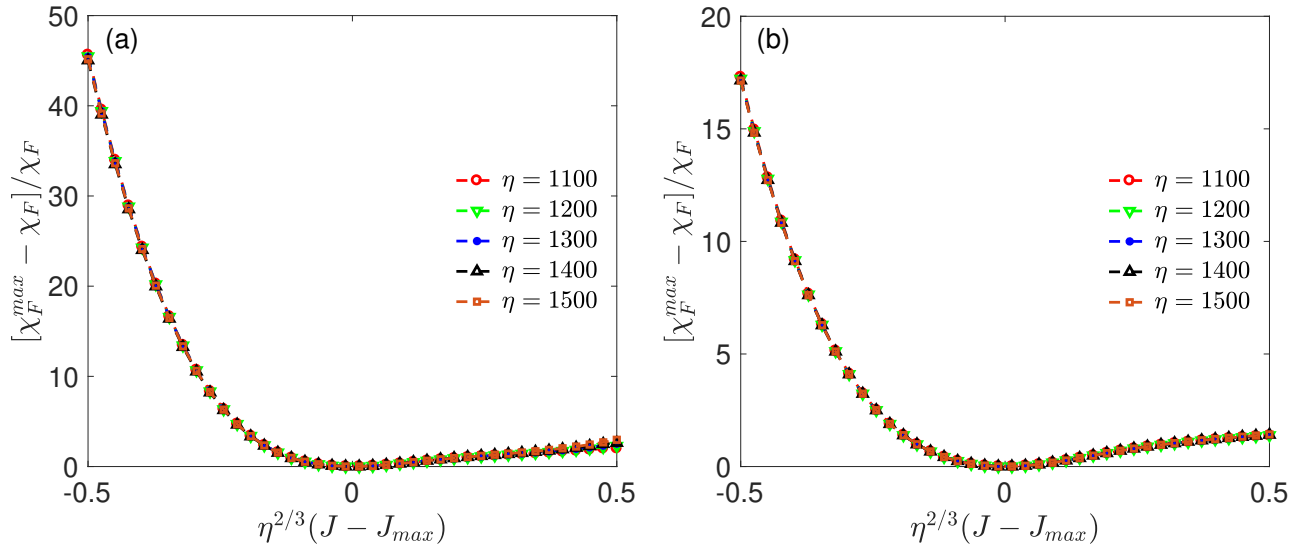


Figure 5: (Color online) Finite-frequency scaling of the rescaled FS according to Eq. (13) with $g = 0.7$ in (a) and with $g = 0.8$ in (b). The colors of the curves correspond to different η . Other involved parameter is $\delta J = 10^{-5}$.

We illustrate the quantum scaling behavior by the rescaled FS [54, 62]

$$\frac{\chi_F^{max} - \chi_F}{\chi_F} = f \left[\eta^{1/\nu} (J - J_{max}) \right]. \quad (13)$$

The fraction $(\chi_F^{max} - \chi_F)/\chi_F$ has reduced the leading coefficient $\eta^{2/\nu}$ in Eq. (12), making itself be a universal function of the rescaled control parameter $\eta^{1/\nu}(J - J_{max})$. After taking $\delta J = 10^{-5}$, the rescaled FS of cases $g = 0.7$ and $g = 0.8$

for different η has been presented in Fig. 5(a) and 5(b), respectively. Intuitively, the rescaled FS with various η collapse onto a single curve with CLCE $\nu = 3/2$, signaling the same universal class in the single Rabi model, RD model, Dicke model, and the LMG model.

IV. SUMMARY

In conclusion, an inter-cavity-hopping-parameter driven SPT in the Rabi-dimer model has been studied. We have shown that the superradiance transition can be characterized by the GS energy and the GS photon population, as well as the GS expectation value of the squared anti-symmetric normal mode. In the normal phase, we find that the GS energy is invariant as the frequency ratio increases and no photon population can be observed in the ground state. On the contrary, in the superradiant phase, accompanied by the decrease of the GS energy, macroscopic photon excitation emerges. Moreover, the trend of the GS expectation value of the anti-symmetric mode is similar to that of the GS photon population. In the normal phase, the expectation value approaches zero, whereas it becomes a finite number when the system is in the superradiant phase. After performing the scaling analysis on the fidelity susceptibility, we verified that such an SPT belongs to the same universal class as the phase transition in the single Rabi model, RD model, Dicke model, and the LMG model. Our study promotes a further understanding of the SPT in the Rabi-dimer model. We notice that recently there is a work on the experimental realization of the Rabi-Hubbard model with trapped ions [64]. The Rabi-dimer model can be regarded as a minimal multi-cavity system of the Rabi-Hubbard model. We hope our theoretical finding that the quantum critical behavior driven by the inter-cavity coupling can be confirmed by the quantum simulation with trapped ions.

ACKNOWLEDGMENTS

We thank Maoxin Liu, Wen-long You, and Liwei Duan for their insightful discussions and acknowledge Dr. Akhtar Naeem for his effort in polishing the English. This work is supported by the NSFC under Grants No. 11835011 and No. 12174346.

Appendix A: Results of $g = 0.5$

In this appendix, we present the numerical analysis about the case with $g = 0.5$ and $N_{cut} = 180$. Figure 6(a) plots the GS energy E_0 as a function of the cavity-coupling parameter J . Intuitively, $E_0 \approx -\eta$ before the SPT, and it tends to lower values when the system enters into the superradiant phase. In analogy to the cases for $g = 0.7$ and $g = 0.8$, there are macroscopic excitation photons accompanying the decrease of E_0 , indicating the occurrence of SPT (see Fig. 6(b)). The trend of the GS expectation value of the squared anti-symmetric normal mode $\langle x_-^2 \rangle$ is similar to that of the GS photon population. As the Fig. 6(c) shows, when the system is in the normal phase, $\langle x_-^2 \rangle \approx 0$, whereas it goes to finite values when J crosses the critical point. To investigate the quantum criticality of this case, we calculate the FS according to Eq. (10) for various η , which are shown in Fig. 6(d) (where the inset represents the zoom around the peak of χ_F/η). We can see that, when η gets larger, the peak of χ_F/η gets larger and the corresponding J_{max} is closer to the theoretical value $J_c^{g=0.5} = 0.375$. The data fitting of χ_F^{max} is presented in Fig. 6(e). The red circles denote the numerically obtained data. The black solid line is the fitting curve of these data, whose slope presents the scaling exponent of FS $\mu = 1.308 \pm 0.001$. Furthermore, we calculate the CLCE by $\mu = 2/\nu$, and obtain the CLCE is $\nu = 1.529 \pm 0.001$, which is closer to the theoretical value $\nu = 3/2$ than those of the $N_{cut} = 80$ cases. Although there is a slight deviation between the obtained ν and the theoretical value $\nu = 3/2$, the rescaled FS plotted in Fig. 6(f) with various η show that they all collapse onto a single curve with CLCE $\nu = 3/2$.

-
- [1] R. H. Dicke, *Coherence in spontaneous radiation processes*, Phys. Rev. 93 (1954) 99–110. doi:10.1103/PhysRev.93.99. URL <https://link.aps.org/doi/10.1103/PhysRev.93.99>
 - [2] N. Skribanowitz, I. P. Herman, J. C. MacGillivray, M. S. Feld, *Observation of dicke superradiance in optically pumped hf gas*, Phys. Rev. Lett. 30 (1973) 309–312. doi:10.1103/PhysRevLett.30.309. URL <https://link.aps.org/doi/10.1103/PhysRevLett.30.309>
 - [3] M. Gross, C. Fabre, P. Pillet, S. Haroche, *Observation of near-infrared dicke superradiance on cascading transitions in atomic sodium*, Phys. Rev. Lett. 36 (1976) 1035–1038. doi:10.1103/PhysRevLett.36.1035. URL <https://link.aps.org/doi/10.1103/PhysRevLett.36.1035>

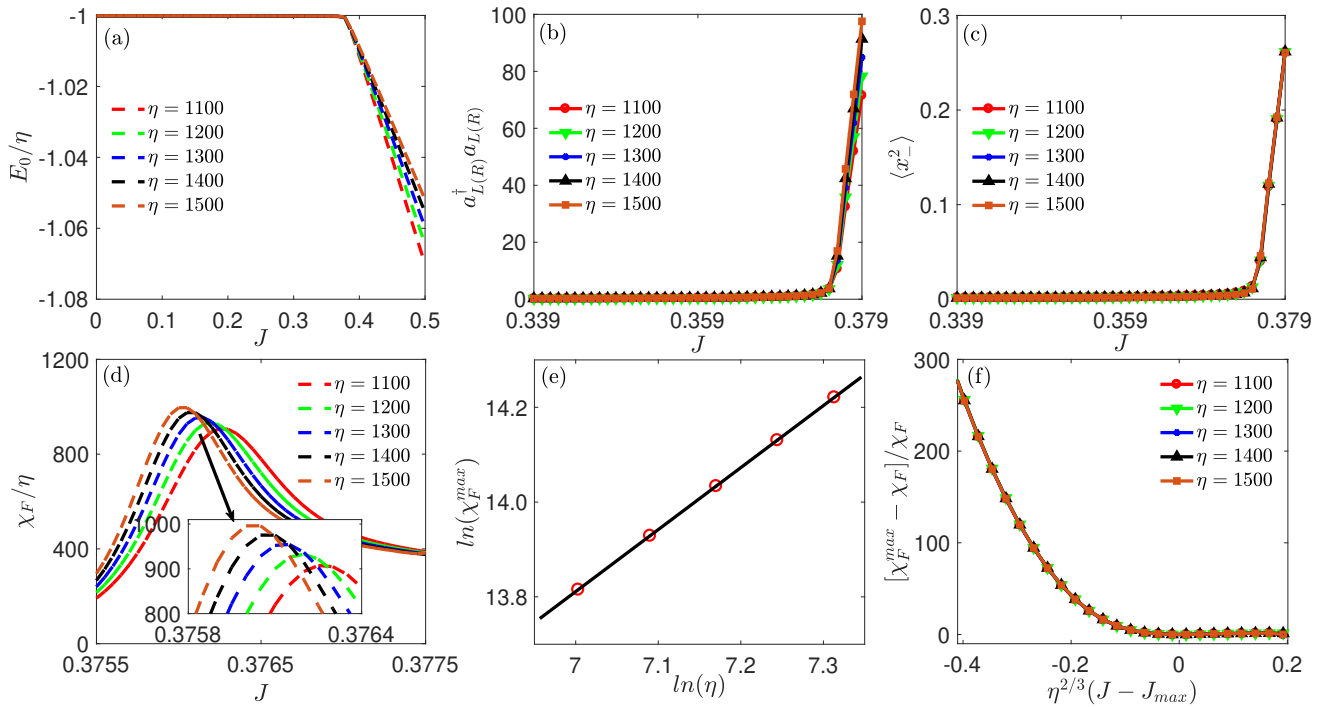


Figure 6: (Color online) (a) GS energy E_0 as a function of J for different η . (b) GS photon population $\langle a_{L(R)}^\dagger a_{L(R)} \rangle$ versus J for different η . (c) GS expectation value of squared anti-symmetric normal mode $\langle x_-^2 \rangle$ varies with J for different η . (d) The fidelity susceptibility χ_F versus J for different η . The inset represents the zoom around the peak of χ_F/η . The involved parameter is $\delta J = 5 \times 10^{-5}$. (e) Finite-frequency scaling analysis of the maximal χ_F with $\delta J = 10^{-5}$ (numerically obtained data are show with red circles). The slope of the fitting curve (black line) presents the scaling exponent of the fidelity susceptibility $\mu = 1.308 \pm 0.001$. (f) The rescaled FS as a function of J for different η . The involved parameter is $\delta J = 10^{-5}$.

- [4] H. M. Gibbs, Q. H. F. Vreken, H. M. J. Hiksloops, [Single-pulse superfluorescence in cesium](#), Phys. Rev. Lett. 39 (1977) 547–550. doi:10.1103/PhysRevLett.39.547. URL <https://link.aps.org/doi/10.1103/PhysRevLett.39.547>
- [5] M. Gross, S. Haroche, [Superradiance: An essay on the theory of collective spontaneous emission](#), Physics Reports 93 (1982) 301–396.
- [6] M. O. Araújo, I. Krešić, R. Kaiser, W. Guerin, [Superradiance in a large and dilute cloud of cold atoms in the linear-optics regime](#), Phys. Rev. Lett. 117 (2016) 073002. doi:10.1103/PhysRevLett.117.073002. URL <https://link.aps.org/doi/10.1103/PhysRevLett.117.073002>
- [7] S. J. Roof, K. J. Kemp, M. D. Havey, I. M. Sokolov, [Observation of single-photon superradiance and the cooperative lamb shift in an extended sample of cold atoms](#), Phys. Rev. Lett. 117 (2016) 073003. doi:10.1103/PhysRevLett.117.073003. URL <https://link.aps.org/doi/10.1103/PhysRevLett.117.073003>
- [8] D. Das, B. Lemberger, D. D. Yavuz, [Subradiance and superradiance-to-subradiance transition in dilute atomic clouds](#), Phys. Rev. A 102 (2020) 043708. doi:10.1103/PhysRevA.102.043708. URL <https://link.aps.org/doi/10.1103/PhysRevA.102.043708>
- [9] R. Röhlsberger, K. Schlage, B. Sahoo, S. Couet, R. Ruffer, [Collective lamb shift in single-photon superradiance](#), Science 328 (5983) (2010) 1248–1251. arXiv:<https://www.science.org/doi/pdf/10.1126/science.1187770>, doi:10.1126/science.1187770. URL <https://www.science.org/doi/abs/10.1126/science.1187770>
- [10] M. Gross, P. Goy, C. Fabre, S. Haroche, J. M. Raimond, [Maser oscillation and microwave superradiance in small systems of rydberg atoms](#), Phys. Rev. Lett. 43 (1979) 343–346. doi:10.1103/PhysRevLett.43.343. URL <https://link.aps.org/doi/10.1103/PhysRevLett.43.343>
- [11] T. Wang, S. F. Yelin, R. Côté, E. E. Eyler, S. M. Farooqi, P. L. Gould, M. Kostrun, D. Tong, D. Vranceanu, [Superradiance in ultracold rydberg gases](#), Phys. Rev. A 75 (2007) 033802. doi:10.1103/PhysRevA.75.033802. URL <https://link.aps.org/doi/10.1103/PhysRevA.75.033802>
- [12] J. O. Day, E. Brekke, T. G. Walker, [Dynamics of low-density ultracold rydberg gases](#), Phys. Rev. A 77 (2008) 052712. doi:10.1103/PhysRevA.77.052712. URL <https://link.aps.org/doi/10.1103/PhysRevA.77.052712>
- [13] D. D. Grimes, S. L. Coy, T. J. Barnum, Y. Zhou, S. F. Yelin, R. W. Field, [Direct single-shot observation of millimeter-wave superradiance in rydberg-rydberg transitions](#), Phys. Rev. A 95 (2017) 043818. doi:10.1103/PhysRevA.95.043818.

- URL <https://link.aps.org/doi/10.1103/PhysRevA.95.043818>
- [14] J. Mlynek, A. Abdumalikov, C. Eichler, A. Wallraff, Observation of dicke superradiance for two artificial atoms in a cavity with high decay rate, *Nat. Commun* 5 (2014) 5186. doi:10.1038/ncomms6186.
URL <https://doi.org/10.1038/ncomms6186>
- [15] M. Scheibner, T. Schmidt, L. Worschech, A. Forchel, G. Bacher, T. Passow, D. Hommel, Superradiance of quantum dots, *Nat. Phys.* 3 (2007) 106. doi:10.1038/nphys494.
URL <https://doi.org/10.1038/nphys494>
- [16] K. Cong, Q. Zhang, Y. Wang, G. T. Noe, A. Belyanin, J. Kono, Dicke superradiance in solids, *J. Opt. Soc. Am. B* 33 (7) (2016) C80–C101. doi:10.1364/JOSAB.33.000C80.
URL <http://opg.optica.org/josab/abstract.cfm?URI=josab-33-7-C80>
- [17] D. Meiser, J. Ye, D. R. Carlson, M. J. Holland, Prospects for a millihertz-linewidth laser, *Phys. Rev. Lett.* 102 (2009) 163601. doi:10.1103/PhysRevLett.102.163601.
URL <https://link.aps.org/doi/10.1103/PhysRevLett.102.163601>
- [18] T. Maier, S. Kraemer, L. Ostermann, H. Ritsch, A superradiant clock laser on a magic wavelength optical lattice, *Opt. Express* 22 (11) (2014) 13269–13279. doi:10.1364/OE.22.013269.
URL <http://opg.optica.org/oe/abstract.cfm?URI=oe-22-11-13269>
- [19] J. G. Bohnet, Z. Chen, J. M. Weiner, D. Meiser, M. J. Holland, J. K. Thompson, A steady-state superradiant laser with less than one intracavity photon, *Nature* 484 (2012) 78–81. doi:10.1038/nature10920.
URL <https://doi.org/10.1038/nature10920>
- [20] M. A. Norcia, J. K. Thompson, Cold-strontium laser in the superradiant crossover regime, *Phys. Rev. X* 6 (2016) 011025. doi:10.1103/PhysRevX.6.011025.
URL <https://link.aps.org/doi/10.1103/PhysRevX.6.011025>
- [21] M. A. Norcia, J. R. K. Cline, J. A. Muniz, J. M. Robinson, R. B. Hutson, A. Goban, G. E. Marti, J. Ye, J. K. Thompson, Frequency measurements of superradiance from the strontium clock transition, *Phys. Rev. X* 8 (2018) 021036. doi:10.1103/PhysRevX.8.021036.
URL <https://link.aps.org/doi/10.1103/PhysRevX.8.021036>
- [22] T. Laske, H. Winter, A. Hemmerich, Pulse delay time statistics in a superradiant laser with calcium atoms, *Phys. Rev. Lett.* 123 (2019) 103601. doi:10.1103/PhysRevLett.123.103601.
URL <https://link.aps.org/doi/10.1103/PhysRevLett.123.103601>
- [23] S. A. Schäffer, M. Tang, M. R. Henriksen, A. A. Jørgensen, B. T. R. Christensen, J. W. Thomsen, Lasing on a narrow transition in a cold thermal strontium ensemble, *Phys. Rev. A* 101 (2020) 013819. doi:10.1103/PhysRevA.101.013819.
URL <https://link.aps.org/doi/10.1103/PhysRevA.101.013819>
- [24] I. I. Rabi, On the process of space quantization, *Phys. Rev.* 49 (1936) 324–328. doi:10.1103/PhysRev.49.324.
URL <https://link.aps.org/doi/10.1103/PhysRev.49.324>
- [25] P. Meystre, *Quantum Optics*, Springer, Cham, 2021. doi:10.1007/978-3-030-76183-7.
- [26] M. Kus, M. Lewenstein, Exact isolated solutions for the class of quantum optical systems, *Journal of Physics A: Mathematical and General* 19 (2) (1986) 305. doi:10.1088/0305-4470/19/2/023.
URL <https://doi.org/10.1088/0305-4470/19/2/023>
- [27] C. Emary, R. F. Bishop, Bogoliubov transformations and exact isolated solutions for simple nonadiabatic hamiltonians, *Journal of Mathematical Physics* 43 (8) (2002) 3916–3926. doi:10.1063/1.1490406.
URL <https://doi.org/10.1063/1.1490406>
- [28] I. D. Feranchuk, L. I. Komarov, A. P. Ulyanenko, Two-level system in a one-mode quantum field: numerical solution on the basis of the operator method, *Journal of Physics A: Mathematical and General* 29 (14) (1996) 4035–4047. doi:10.1088/0305-4470/29/14/026.
URL <https://doi.org/10.1088/0305-4470/29/14/026>
- [29] E. K. Irish, Generalized rotating-wave approximation for arbitrarily large coupling, *Phys. Rev. Lett.* 99 (2007) 173601. doi:10.1103/PhysRevLett.99.173601.
URL <https://link.aps.org/doi/10.1103/PhysRevLett.99.173601>
- [30] S. Ashhab, F. Nori, Qubit-oscillator systems in the ultrastrong-coupling regime and their potential for preparing nonclassical states, *Phys. Rev. A* 81 (2010) 042311. doi:10.1103/PhysRevA.81.042311.
URL <https://link.aps.org/doi/10.1103/PhysRevA.81.042311>
- [31] C. Gan, H. Zheng, Dynamics of a two-level system coupled to a quantum oscillator: transformed rotating-wave approximation, *Eur. Phys. J. D* 59 (2010) 473. doi:10.1140/epjd/e2010-00182-8.
URL <https://doi.org/10.1140/epjd/e2010-00182-8>
- [32] J. Hausinger, M. Grifoni, Qubit-oscillator system: An analytical treatment of the ultrastrong coupling regime, *Phys. Rev. A* 82 (2010) 062320. doi:10.1103/PhysRevA.82.062320.
URL <https://link.aps.org/doi/10.1103/PhysRevA.82.062320>
- [33] V. V. Albert, G. D. Scholes, P. Brumer, Symmetric rotating-wave approximation for the generalized single-mode spin-boson system, *Phys. Rev. A* 84 (2011) 042110. doi:10.1103/PhysRevA.84.042110.
URL <https://link.aps.org/doi/10.1103/PhysRevA.84.042110>
- [34] D. Braak, Integrability of the rabi model, *Phys. Rev. Lett.* 107 (2011) 100401. doi:10.1103/PhysRevLett.107.100401.
URL <https://link.aps.org/doi/10.1103/PhysRevLett.107.100401>
- [35] V. Bargmann, On a hilbert space of analytic functions and an associated integral transform, *Comm. Pure Appl. Math.* 14 (1961) 187. doi:10.1002/cpa.3160140303.

- URL <https://doi.org/10.1002/cpa.3160140303>
- [36] Q.-H. Chen, C. Wang, S. He, T. Liu, K.-L. Wang, Exact solvability of the quantum rabi model using bogoliubov operators, *Phys. Rev. A* 86 (2012) 023822. doi:10.1103/PhysRevA.86.023822.
URL <https://link.aps.org/doi/10.1103/PhysRevA.86.023822>
- [37] L. Duan, S. He, D. Braak, Q.-H. Chen, Solution of the two-mode quantum rabi model using extended squeezed states, *EPL (Europhysics Letters)* 112 (3) (2015) 34003. doi:10.1209/0295-5075/112/34003.
URL <https://doi.org/10.1209/0295-5075/112/34003>
- [38] L. Duan, Y.-F. Xie, D. Braak, Q.-H. Chen, Two-photon rabi model: analytic solutions and spectral collapse, *Journal of Physics A: Mathematical and Theoretical* 49 (46) (2016) 464002. doi:10.1088/1751-8113/49/46/464002.
URL <https://doi.org/10.1088/1751-8113/49/46/464002>
- [39] D. Braak, Q.-H. Chen, M. T. Batchelor, E. Solano, Semi-classical and quantum rabi models: in celebration of 80 years, *Journal of Physics A: Mathematical and Theoretical* 49 (30) (2016) 300301. doi:10.1088/1751-8113/49/30/300301.
URL <https://doi.org/10.1088/1751-8113/49/30/300301>
- [40] Q. Xie, H. Zhong, M. T. Batchelor, C. Lee, The quantum rabi model: solution and dynamics, *Journal of Physics A: Mathematical and Theoretical* 50 (11) (2017) 113001. doi:10.1088/1751-8121/aa5a65.
URL <https://doi.org/10.1088/1751-8121/aa5a65>
- [41] P. Forn-Díaz, L. Lamata, E. Rico, J. Kono, E. Solano, Ultrastrong coupling regimes of light-matter interaction, *Rev. Mod. Phys.* 91 (2019) 025005. doi:10.1103/RevModPhys.91.025005.
URL <https://link.aps.org/doi/10.1103/RevModPhys.91.025005>
- [42] M. S. Choi, Exotic quantum states of circuit quantum electrodynamics in the ultra-strong coupling regime, doi:10.1002/qute.202000085.
URL <https://link.aps.org/doi/10.1002/qute.202000085>
- [43] M.-J. Hwang, R. Puebla, M. B. Plenio, Quantum phase transition and universal dynamics in the rabi model, *Phys. Rev. Lett.* 115 (2015) 180404. doi:10.1103/PhysRevLett.115.180404.
URL <https://link.aps.org/doi/10.1103/PhysRevLett.115.180404>
- [44] M.-J. Hwang, M. B. Plenio, Quantum phase transition in the finite jaynes-cummings lattice systems, *Phys. Rev. Lett.* 117 (2016) 123602. doi:10.1103/PhysRevLett.117.123602.
URL <https://link.aps.org/doi/10.1103/PhysRevLett.117.123602>
- [45] M. Liu, S. Chesi, Z.-J. Ying, X. Chen, H.-G. Luo, H.-Q. Lin, Universal scaling and critical exponents of the anisotropic quantum rabi model, *Phys. Rev. Lett.* 119 (2017) 220601. doi:10.1103/PhysRevLett.119.220601.
URL <https://link.aps.org/doi/10.1103/PhysRevLett.119.220601>
- [46] M.-J. Hwang, M. S. Kim, M.-S. Choi, Recurrent delocalization and quasiequilibration of photons in coupled systems in circuit quantum electrodynamics, *Phys. Rev. Lett.* 116 (2016) 153601. doi:10.1103/PhysRevLett.116.153601.
URL <https://link.aps.org/doi/10.1103/PhysRevLett.116.153601>
- [47] B.-B. Wei, X.-C. Lv, Fidelity susceptibility in the quantum rabi model, *Phys. Rev. A* 97 (2018) 013845. doi:10.1103/PhysRevA.97.013845.
URL <https://link.aps.org/doi/10.1103/PhysRevA.97.013845>
- [48] Y. Wang, M. Liu, W.-L. You, S. Chesi, H.-G. Luo, H.-Q. Lin, Resilience of the superradiant phase against a^2 effects in the quantum rabi dimer, *Phys. Rev. A* 101 (2020) 063843. doi:10.1103/PhysRevA.101.063843.
URL <https://link.aps.org/doi/10.1103/PhysRevA.101.063843>
- [49] B.-B. Mao, L. Li, W.-L. You, M. Liu, Superradiant phase transition in quantum rabi dimer with staggered couplings, *Physica A: Statistical Mechanics and its Applications* 564 (C) (2021) S0378437120308323.
URL <https://EconPapers.repec.org/RePEc:eee:phsmap:v:564:y:2021:i:c:s0378437120308323>
- [50] J. Vidal, S. Dusuel, Finite-size scaling exponents in the dicke model, *Europhysics Letters (EPL)* 74 (5) (2006) 817–822. doi:10.1209/epl/i2006-10041-9.
URL <https://doi.org/10.1209/epl/i2006-10041-9>
- [51] T. Liu, Y.-Y. Zhang, Q.-H. Chen, K.-L. Wang, Large- n scaling behavior of the ground-state energy, fidelity, and the order parameter in the dicke model, *Phys. Rev. A* 80 (2009) 023810. doi:10.1103/PhysRevA.80.023810.
URL <https://link.aps.org/doi/10.1103/PhysRevA.80.023810>
- [52] S. Dusuel, J. Vidal, Finite-size scaling exponents of the lipkin-meshkov-glick model, *Phys. Rev. Lett.* 93 (2004) 237204. doi:10.1103/PhysRevLett.93.237204.
URL <https://link.aps.org/doi/10.1103/PhysRevLett.93.237204>
- [53] S. Dusuel, J. Vidal, Continuous unitary transformations and finite-size scaling exponents in the lipkin-meshkov-glick model, *Phys. Rev. B* 71 (2005) 224420. doi:10.1103/PhysRevB.71.224420.
URL <https://link.aps.org/doi/10.1103/PhysRevB.71.224420>
- [54] H.-M. Kwok, W.-Q. Ning, S.-J. Gu, H.-Q. Lin, Quantum criticality of the lipkin-meshkov-glick model in terms of fidelity susceptibility, *Phys. Rev. E* 78 (2008) 032103. doi:10.1103/PhysRevE.78.032103.
URL <https://link.aps.org/doi/10.1103/PhysRevE.78.032103>
- [55] M. A. Nielsen, I. L. Chuang, *Quantum Computation and Quantum Information: 10th Anniversary Edition*, Cambridge University Press, 2010. doi:10.1017/CB09780511976667.
- [56] H. T. Quan, Z. Song, X. F. Liu, P. Zanardi, C. P. Sun, Decay of loschmidt echo enhanced by quantum criticality, *Phys. Rev. Lett.* 96 (2006) 140604. doi:10.1103/PhysRevLett.96.140604.
URL <https://link.aps.org/doi/10.1103/PhysRevLett.96.140604>
- [57] P. Zanardi, N. Paunković, Ground state overlap and quantum phase transitions, *Phys. Rev. E* 74 (2006) 031123. doi:

- 10.1103/PhysRevE.74.031123.
URL <https://link.aps.org/doi/10.1103/PhysRevE.74.031123>
- [58] S.-J. Gu, Fidelity approach to quantum phase transitions, International Journal of Modern Physics B 24 (23) (2010) 4371–4458. [arXiv:https://doi.org/10.1142/S0217979210056335](https://arxiv.org/abs/https://doi.org/10.1142/S0217979210056335), [doi:10.1142/S0217979210056335](https://doi.org/10.1142/S0217979210056335).
URL <https://doi.org/10.1142/S0217979210056335>
- [59] W.-L. You, Y.-W. Li, S.-J. Gu, Fidelity, dynamic structure factor, and susceptibility in critical phenomena, Phys. Rev. E 76 (2007) 022101. [doi:10.1103/PhysRevE.76.022101](https://doi.org/10.1103/PhysRevE.76.022101).
URL <https://link.aps.org/doi/10.1103/PhysRevE.76.022101>
- [60] P. Zanardi, P. Giorda, M. Cozzini, Information-theoretic differential geometry of quantum phase transitions, Phys. Rev. Lett. 99 (2007) 100603. [doi:10.1103/PhysRevLett.99.100603](https://doi.org/10.1103/PhysRevLett.99.100603).
URL <https://link.aps.org/doi/10.1103/PhysRevLett.99.100603>
- [61] L. Campos Venuti, P. Zanardi, Quantum critical scaling of the geometric tensors, Phys. Rev. Lett. 99 (2007) 095701. [doi:10.1103/PhysRevLett.99.095701](https://doi.org/10.1103/PhysRevLett.99.095701).
URL <https://link.aps.org/doi/10.1103/PhysRevLett.99.095701>
- [62] S.-J. Gu, H.-M. Kwok, W.-Q. Ning, H.-Q. Lin, Fidelity susceptibility, scaling, and universality in quantum critical phenomena, Phys. Rev. B 77 (2008) 245109. [doi:10.1103/PhysRevB.77.245109](https://doi.org/10.1103/PhysRevB.77.245109).
URL <https://link.aps.org/doi/10.1103/PhysRevB.77.245109>
- [63] A. F. Albuquerque, F. Alet, C. Sire, S. Capponi, Quantum critical scaling of fidelity susceptibility, Phys. Rev. B 81 (2010) 064418. [doi:10.1103/PhysRevB.81.064418](https://doi.org/10.1103/PhysRevB.81.064418).
URL <https://link.aps.org/doi/10.1103/PhysRevB.81.064418>
- [64] Q.-X. Mei, B.-W. Li, Y.-K. Wu, M.-L. Cai, Y. Wang, L. Yao, Z.-C. Zhou, L.-M. Duan, Experimental realization of the rabi-hubbard model with trapped ions, Phys. Rev. Lett. 128 (2022) 160504. [doi:10.1103/PhysRevLett.128.160504](https://doi.org/10.1103/PhysRevLett.128.160504).
URL <https://link.aps.org/doi/10.1103/PhysRevLett.128.160504>